Title	FDTD modeling of time-modulated resonators-based bandpass filters using modified telegrapher's equations
Authors	Kumar, Anand;Zhang, Zixiao;Sarkar, Debdeep;Nikolaou, Symeon;Vryonides, Photos;Psychogiou, Dimitra
Publication date	2024-07-30
Original Citation	Kumar, A., Zhang, Z., Sarkar, D., Nikolaou, S., Vryonides, P. and Psychogiou, D. (2024) 'FDTD modeling of time-modulated resonators-based bandpass filters using modified telegrapher's equations', 2024 IEEE/MTT-S International Microwave Symposium - IMS 2024, Washington, DC, USA, 16-21 June, pp. 612-615. https://doi.org/10.1109/IMS40175.2024.10600413
Type of publication	Conference item
Link to publisher's version	10.1109/IMS40175.2024.10600413
Rights	© 2024, IEEE. Personal use of this material is permitted. Permission from IEEE must be obtained for all other uses, in any current or future media, including reprinting/republishing this material for advertising or promotional purposes, creating new collective works, for resale or redistribution to servers or lists, or reuse of any copyrighted component of this work in other works.
Download date	2025-04-24 07:29:15
Item downloaded from	https://hdl.handle.net/10468/16254

FDTD Modeling of Time-Modulated Resonators-Based Bandpass Filters using Modified Telegrapher's Equations

Anand Kumar[#$1], Zixiao Zhang[#2], Debdeep Sarkar[$3], Symeon Nikolaou[*4], Photos Vryonides[*5], Dimitra Psychogiou[#6]

[#]Tyndall National Institute, University College Cork, Ireland
[$]Department of Electrical Communication Engineering, Indian Institute of Science, Bengaluru, India
[*]Frederick University, Frederick Research Center, Nicosia, Cyprus
{[1]anandkumar13, [3]debdeep}@iisc.ac.in, [2]zixiao.zhang@tyndall.ie, {[4]s.nikolaou, [5]p.vryonides}@frederick.ac.cy, [6]DPsychogiou@ucc.ie

***Abstract*— This manuscript reports for the first time on a new finite-difference time-domain (FDTD) modeling technique for non-reciprocal bandpass filters (BPFs). The proposed approach is based on modified Telegrapher's equations that are adjusted to facilitate the FDTD modeling of discrete time-invariant and time-variant *L*, *C* components, and *LC* resonators that can be used for the design of RF components. In this paper, this method has been exploited for the design of non-reciprocal BPFs using time-variant resonators. The efficacy of the approach is demonstrated through the modeling of two non-reciprocal filtering examples that are compared with harmonic balance simulations in Keysight ADS. These include a three-pole BPF and a three-pole/two-transmission zero (TZ) non-reciprocal BPF.**

***Keywords*— finite-difference time-domain, FDTD, isolator, filter, non-reciprocity.**

I. Introduction

Non-reciprocal bandpass filters (NR-BPFs) are increasingly being explored due to their potential to: i) reduce the size of the RF front-end by incorporating the co-designed isolator function and to: ii) improve the signal-to-noise ratio by canceling unwanted reflections [1]. While diverse techniques have been developed for incorporating non-reciprocity in BPFs [2], [3], [4], the utilization of time-modulated resonators [5], [6], [7] is among the most promising ones due not requiring external magnetic biasing as is the case in ferrite-based isolators. These time-modulated resonators are formed by a combination of inductors and nonlinear time-dependent capacitors and are typically modeled using harmonic balance (HB) simulations, which are slow, difficult to converge, and hard to optimize due to the large number of variables that contribute to the performance of the NR-BPF [5], [7]. Thus, alternative NR-BPF design techniques are being explored. These include using the spectral admittance matrix (SAM) in [5] and a modified coupling matrix (CM) approach in [6] where the SAM in [5] is incorporated into the CM to generate a spectral CM. However, both of the methods in [5], [6] necessitate rigorous analysis and are constrained by the number of harmonics considered for solving the CMs.

In yet another approach, non-reciprocity in space-time modulated propagation media has been analyzed using the finite-difference time-domain (FDTD) method for acoustic,

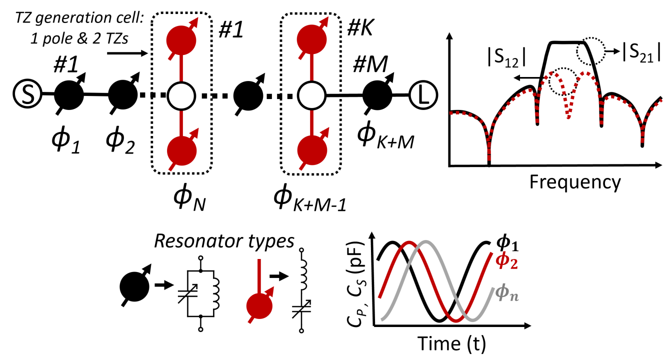

Fig. 1. Generic CRD of an NR-BPF. It comprises of *M* time/modulated in/line resonators and up to *K* time-modulated TZ generation cells. When unmodulated, it exhibits a transfer function shaped by *M*+*K* poles and 2*K* TZs. Non-reciprocity is introduced by modulating the resonators with progressively phase-shifted low-frequency AC signals.

microwave, and optical systems [8], [9], [10]. The FDTD method was used to model the time-varying permittivity of homogeneous dielectric media in [11], [12], [13]. In [14], [15], modified Telegrapher's equations were proposed to model the time-varying transmission lines (TVTLs) of a traveling-wave amplifier. An FDTD method based on the Telegrapher's equations was also presented in [13] to model TVTLs in [13] and in [16] and in [17] time-varying capacitors were added on TLs to demonstrate frequency mixing. However, none of these FDTD methods has been demonstrated for time-variant capacitors and resonators; thus, they aren't yet applicable to the design of NR-BPFs.

Considering the aforementioned limitations, this paper proposes an FDTD modeling method for discrete time-varying capacitors, series-, and parallel-*LC* that can be exploited for the design and analysis of NR-BPFs. It is based on modified Telegrapher equations that use as a basis modified unit cells shaped by incorporating time-variant capacitors on transmission lines (TL). To demonstrate the potential of the proposed method, two different NR-BPF examples, namely a three-pole and a three-pole/two transmission zero (TZ), have been implemented and are compared with HB simulations in ADS, demonstrating an excellent agreement. As opposed to alternative NR-BPF design techniques, the proposed FDTD formulation evaluates the circuit in the time domain while

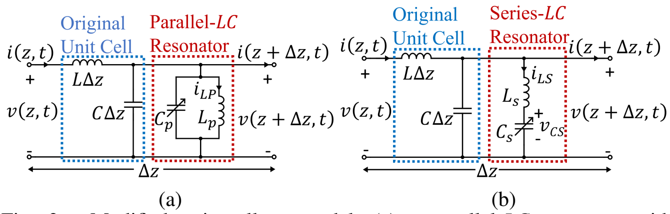

Fig. 2. Modified unit cell to model: (a) a parallel-*LC* resonator with time/variable resonant frequency, and (b) a series-*LC* resonator with time/variable resonant frequency.

considering all higher-order harmonics, distinguishing it from analytical methods [5], [6] and the HB simulations. Thus, it can be scaled to high order and advanced filtering transfer functions without the need to restrict the harmonics, which makes it more accurate and can be readily co-integrated with optimization algorithms. Furthermore, it allows to investigate the performance of NR-BPFs under alternative excitation schemes, which can't be easily implemented in commercially available circuit simulators.

II. Non-Reciprocal Bandpass Filters

A generic block diagram of an NR-BPF is illustrated in Fig. 1. It comprises of M time/modulated in/line resonators and up to K time-modulated transmission-zero (TZ) generation cells cascaded through impedance inverters. When unmodulated, the filter exhibits a transfer function shaped by $M + K$ poles and $2K$ TZs [7]. Non/reciprocity is introduced by modulating the resonators with progressively phase-shifted low-frequency AC signals ($f_{AC} \ll f_{RF}$) that create a time-variable capacitance [5], [6], [7]. To facilitate the analysis of these filters using FDTD, a Telegraph equation-based approach can be considered for the modeling of its key elements, namely the time-variable capacitors, the time/varying parallel or series/type resonators, and the time/invariant inverters, which are described in the next section.

A. Modeling of a time-varying capacitor

Considering that the capacitance C of a capacitor is time-variant, i.e., $C(t)$, then the charge stored at time t will be $q(t) = C(t)v(t)$ and the current through the capacitor can be defined as:

$$i(t) = \frac{dq(t)}{dt} \implies i(t) = \frac{dC(t)v(t)}{dt}. \tag{1}$$

Thus, the finite differences on (1) using the central difference scheme can be defined as in (2) assuming that the capacitor is located at z:

$$i_{k+0.5}^{n+0.5} = \frac{C_k^{n+1}v_k^{n+1} - C_k^n v_k^n}{\Delta t}, \tag{2}$$

where $z = k\Delta z$ and $t = n\Delta t$, Δz and Δt are the discretization in space and time, respectively.

B. Modeling of a parallel-LC in shunt with a TL

Having defined the time-varying capacitor, the time/varying parallel-*LC* resonator (L_p, C_p) can be modeled on the assumption that is meant to be cascaded with an impedance inverter which is a 90° TL, [18], by using a modified unit-cell of a TL and an *LC* tank as shown in Fig. 2(a). In this case, the conventional unit-cell of the low-pass equivalent of a TL has been modified to include an inductor L_p and a time-varying capacitor C_p that can be modeled using (2) and (3)-(4) in [16]. Its corresponding Telegrapher's equations can be modified to:

$$v(z+\Delta z,t) - v(z,t) + L\Delta z\frac{\partial i(z,t)}{\partial t} = 0, \tag{3a}$$

$$i(z,t) - i(z+\Delta z,t) - \frac{\partial C_p(t)v(z+\Delta z,t)}{\partial t} - C\Delta z\frac{\partial v(z+\Delta z,t)}{\partial t} - i_{LP}(z+\Delta z,t) = 0, \tag{3b}$$

where i_{LP} is the current through L_p and is calculated by:

$$i_{LP}(z+\Delta z,t) = \frac{1}{L_p}\int_{t_0}^{t} v(z+\Delta z,t)\partial t + i_{LP}(z+\Delta z,t_0). \tag{3c}$$

Hence, the FDTD update equations are as follows:

$$i_{k+0.5}^{n+0.5} = i_{k+0.5}^{n-0.5} - \left(\frac{\Delta t}{L\Delta z}\right)(v_{k+1}^n - v_k^n), \tag{4a}$$

$$v_k^{n+1} = v_k^n - \left(\frac{\Delta t}{C\Delta z + C_p}\right)(i_{k+0.5}^{n+0.5} - i_{k-0.5}^{n+0.5} + i_{LP,k}^n), \tag{4b}$$

$$i_{LP,k}^{n+1} = i_{LP,k}^n + \left(\frac{\Delta t}{L_p}\right)v_k^n. \tag{4c}$$

C. Modeling of a series-LC Resonator in shunt with a TL

In a similar manner, a series-*LC* resonator (L_s, C_s) can be modeled using the modified unit cell in Fig. 2(b). Its corresponding modified Telegrapher's equations are listed in (5):

$$v(z+\Delta z,t) - v(z,t) + L\Delta z\frac{\partial i(z,t)}{\partial t} = 0, \tag{5a}$$

$$i(z,t) - i(z+\Delta z,t) - C\Delta z\frac{\partial v(z+\Delta z,t)}{\partial t} - i_{LS}(z,t) = 0, \tag{5b}$$

$$L_s\frac{\partial i_{LS}}{\partial t} + v_{CS}(z,t) - v(z+\Delta z,t) = 0, \tag{5c}$$

$$v_{CS}(z,t) = \frac{1}{C_s(t)}\int_{t_0}^{t} i_{LS}(z,t)\partial t + v_{CS}(z,t_0). \tag{5d}$$

Thus, the FDTD update equations are as follows:

$$i_{k+0.5}^{n+0.5} = i_{k+0.5}^{n-0.5} - \left(\frac{\Delta t}{L\Delta z}\right)(v_{k+1}^n - v_k^n), \tag{6a}$$

$$v_k^{n+1} = v_k^n - \left(\frac{\Delta t}{C\Delta z}\right)(i_{k+0.5}^{n+0.5} - i_{k-0.5}^{n+0.5} + i_{LS,k}^{n+1}), \tag{6b}$$

$$i_{LS,k}^{n+1} = i_{LS,k}^n + \left(\frac{\Delta t}{L_s}\right)(v_k^n - v_{CS,k}^n), \tag{6c}$$

$$v_{CS,k}^{n+1} = v_{CS,k}^n + \left(\frac{\Delta t}{C_s}\right)i_{LS,k}^{n+1}. \tag{6d}$$

III. The FDTD Model & S-Parameters Evaluation

To demonstrate the usefulness of the modified unit cells and their corresponding 1D-FDTD update equations in the design of NR-BPFs, two filter design examples are considered and are numerically analyzed in MATLAB. These include a three-pole NR-BPF, i.e., M = 3 and K = 0 in Fig. 1 and a three-pole/two-TZ NR-BPF, i.e., M = 2 and K = 1 in Fig. 1. The simulation space is terminated with a 50 Ω impedance (Z_0) at both Port 1 and 2, and an excitation source is introduced at either of these ports for the calculation of the S-parameters. As the time-varying resonators cause frequency translation and introduce power at the intermodulation frequencies (IF), the wideband calculation of the S-parameters in FDTD using a Sinc/Gaussian pulse fails,

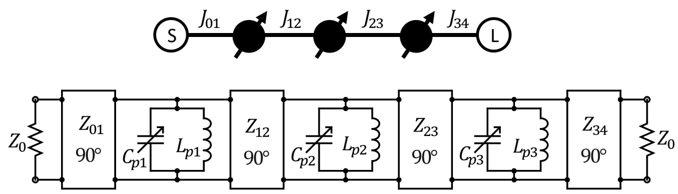

Fig. 3. CRD and equivalent circuit of a three-pole BPFI comprising of three in-series cascaded parallel *LC*-resonators and three impedance inverters.

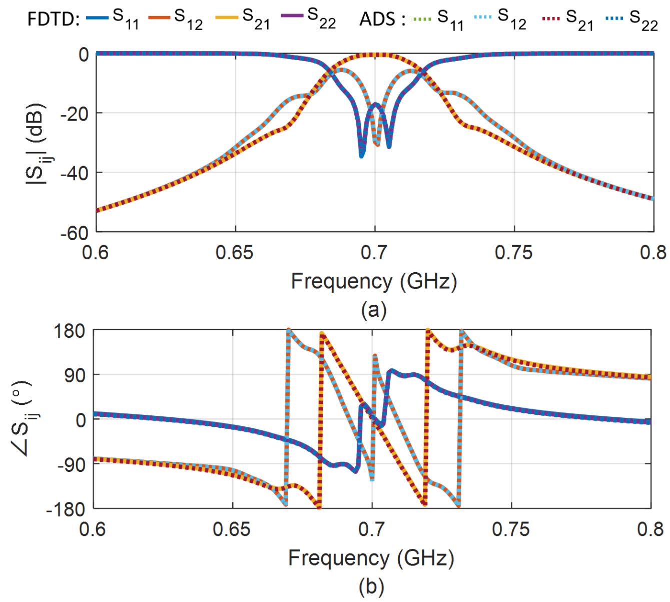

Fig. 4. S-parameter response of the three-pole NR-BPF calculated using the proposed 1D-FDTD method and HB simulations in ADS for the NR-BPF in Fig. 3. (a) Magnitude. (b) Phase.

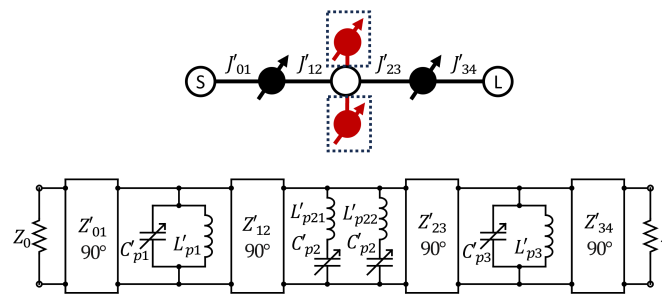

Fig. 5. CRD and equivalent circuit of the three-pole/two-TZ NR-BPF comprising two in-line resonators and one TZ-generation cell.

and hence S-parameters for each frequency must be evaluated individually. Therefore, the excitation is a sinusoidal source of frequency f_{in}, and the FDTD model is simulated for each f_{in} for which the S-parameter is to be extracted. The voltages (V_i) and currents (I_i) at each port (i = 1, 2) are recorded for each f_{in} to calculate the auxiliary parameters a_i and b_i that are defined as:

$$a_i = \frac{V_i + Z_0 I_i}{2\sqrt{Z_0}}, \quad b_i = \frac{V_i - Z_0 I_i}{2\sqrt{Z_0}} \tag{7}$$

Then, $S_{ij,f_{in}} = \left.\frac{b_{i,f_{in}}}{a_{j,f_{in}}}\right|_{a_i=0}$ gives the S-parameters at f_{in}, where $a_{i,f_{in}}$ and $b_{i,f_{in}}$ are the values of the auxiliary parameters at f_{in}.

A. Example 1: Three-pole NR-BPF

The coupling routing diagram (CRD) and circuit equivalent of the three-pole NR-BPF are shown in Fig. 3. It comprises three in-line resonators (M = 3 in Fig. 1) that include time/varying capacitors whose capacitance is modulated by progressively phase shifted AC signals [5]. The unit cell in Fig. 2(a) is used to model the time-varying parallel-*LC* resonators, and the values for v_k^n and i_k^n at the resonators are updated using (4). The admittance inverters (J) are modeled using 90° TL ($Z = J^{-1}\Omega$) and are implemented using (3)-(4) in [16]. The BPF is designed for a centre frequency f_{cen} of 700 MHz and fractional bandwidth (FBW) of 3% using the design method in [5], leading to the following circuit-element values: Z_{01} = Z_{34} = 56.81 Ω, Z_{12} = Z_{23} = 73.46 Ω, L_{p1} = L_{p2} = L_{p3} = 0.517 nH, and where C_0 = 100 pF. To introduce non-reciprocity, the parallel capacitors of each resonator are modeled as follows:

$$C_{pk} = C_0(1 + \zeta cos(2\pi f_m t + (k-1)\phi_1)), \ k = 1, 2, 3. \tag{8}$$

The modulation index (ζ) modulation frequency (f_m) and the phase offset (ϕ_1) are selected as 0.045, 17 MHz and 65° respectively to achieve maximum isolation at f_{cen}.

The obtained S-parameters from the 1D-FDTD model are provided in Fig. 4 and are compared against HB simulations in Keysight ADS in terms of magnitude and phase. They appear to be in excellent agreement, successfully validating the proposed modified 1D-FDTD method. It should be noted that for the ADS simulations up to 8^{th} order harmonics are considered based on the convergence criteria in [5].

B. Example 2: Three-pole/two-TZ NR-BPF

A second example case of a three-pole/two-TZ (M = 2, K = 1 in Fig. 1) BPF whose CRD and practical validation were introduced in [7] and are also shown in Fig. 5. In this case, the parallel-*LC* resonators are modeled by the unit cell in Fig. 2(a) and the series-*LC* resonators by the unit cell in Fig. 2(b). for the following parameters: Z'_{01} = 120.74 Ω, Z'_{12} = 108.67 Ω, Z'_{23} = 54.65 Ω, Z'_{34} = 45.34 Ω, L'_{p1} = L'_{p3} = 16.29 nH, L'_{p21} = 46 nH, L'_{p22} = 24.45 nH, where C'_0 = 17.28 pF ξ_1 = ξ_3 = 0.108, ξ_2 = 0.05, f_m = 16 MHz, ϕ_2 = 60° and

$$C'_{pk} = C'_0(1 + \xi_k cos(2\pi f_m t + (k-1)\phi_2)), \ k = 1, 2, 3. \tag{9}$$

that have been selected for a passband centered at 300 MHz, with FBW of 13% and two TZs located at 262.4 and 342.8 MHz.

The obtained S-parameters from the 1D-FDTD model are provided in Fig. 6 and are furthermore compared with HB simulations in Keysight ADS. They also appear to be in excellent agreement, successfully validating the proposed modified 1D-FDTD method. As an additional advantage to be highlighted, the suggested FDTD model enables testing of the BPFs with real-time input signals, whether periodic or aperiodic, in the time domain. In contrast, the use of HB is restricted to quasi-periodic signals that can be represented as a superposition of a limited number (M) of discrete tones. As M

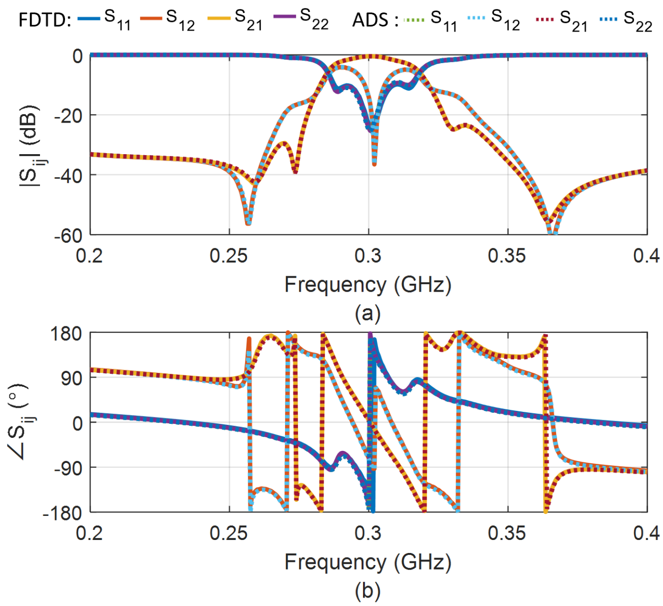

Fig. 6. S-parameter response of the three-pole/two-TZ NR-BPF calculated using the proposed 1D-FDTD method and HB simulations in ADS for the NR-BPF in Fig. 5. (a) Magnitude. (b) Phase.

increases, the required internal memory becomes impractical due to the growth of the internal matrix size [19]. In contrast, the proposed FDTD model overcomes these limitations and can effectively manage arbitrary signals for both source and modulation without such constraints.

IV. Conclusion

In summary, this paper introduced for the first time a robust FDTD model for NR-BPFs by incorporating lumped time-varying capacitors and resonators on a TL. To demonstrate the validity of the proposed method, two filter design cases were considered at 300 MHz and 700 MHz that showed excellent agreement with harmonic balance simulations in a commercially available simulator. This work makes a significant contribution through the introduction of a specialized method for calculating S-parameters, designed specifically for circuits with time-varying components. This method is particularly valuable for (NR-BPFs), which pose challenges in design when using commercially available tools. Specifically, the FDTD formulation evaluates the circuit in the time domain, distinguishing it from other methods and affirming its accuracy.

Acknowledgment

This work has received support from Science Foundation Ireland (SFI) project No. 20/RP/8334, the Science and Engineering Research Board (SERB), Department of Science & Technology, Government of India under grant SRG/2021/000831, and the Prime Minister's Research Fellowship (PMRF), Ministry of Education, Government of India under grant TF/PMRF-22-3965. Additionally, it was partially funded by the Republic of Cyprus through the SMALL SCALE INFRASTRUCTURES/1222/0087 LARISSA-6G project under the Cohesion Policy Funds 'THALEIA 2021-2027' with EU co-funding, and by the Recovery and Resilience Facility of the NextGenerationEU instrument, for Cyprus under the project CODEVELOP-GT/0322/0081 (REALISATION-GREEN-CLOUD).

References

[1] P. Dutta, G. A. Kumar, G. Ram, and D. S. Varma, "Spatiotemporal nonreciprocal filters: Theoretical concepts and literature review," *IEEE Microwave Magazine*, vol. 23, no. 6, pp. 85–101, 2022.

[2] J. Wu, X. Yang, S. Beguhn, J. Lou, and N. X. Sun, "Nonreciprocal tunable low-loss bandpass filters with ultra-wideband isolation based on magnetostatic surface wave," *IEEE Transactions on Microwave Theory and Techniques*, vol. 60, no. 12, pp. 3959–3968, 2012.

[3] X.-H. Li, H.-M. Zhou, Q.-s. Zhang, and W.-W. Hu, "Lumped modeling with circuit elements for nonreciprocal magnetoelectric tunable band-pass filter," *Chinese Physics B*, vol. 25, no. 11, p. 117505, 2016.

[4] M. Ghatge, G. Walters, T. Nishida, and R. Tabrizian, "A non-reciprocal filter using asymmetrically transduced micro-acoustic resonators," *IEEE Electron Device Letters*, vol. 40, no. 5, pp. 800–803, 2019.

[5] X. Wu, X. Liu, M. D. Hickle, D. Peroulis, J. S. Gómez-Díaz, and A. Á. Melcón, "Isolating bandpass filters using time-modulated resonators," *IEEE Transactions on Microwave Theory and Techniques*, vol. 67, no. 6, pp. 2331–2345, 2019.

[6] A. Alvarez-Melcon, X. Wu, J. Zang, X. Liu, and J. S. Gomez-Diaz, "Coupling matrix representation of nonreciprocal filters based on time-modulated resonators," *IEEE Transactions on Microwave Theory and Techniques*, vol. 67, no. 12, pp. 4751–4763, 2019.

[7] D. Simpson and D. Psychogiou, "Fully-reconfigurable non-reciprocal bandpass filters," in *2020 IEEE/MTT-S International Microwave Symposium (IMS)*. IEEE, 2020, pp. 807–810.

[8] J. Li, C. Shen, X. Zhu, Y. Xie, and S. A. Cummer, "Nonreciprocal sound propagation in space-time modulated media," *Physical Review B*, vol. 99, no. 14, p. 144311, 2019.

[9] S. Taravati and C. Caloz, "Mixer-duplexer-antenna leaky-wave system based on periodic space-time modulation," *IEEE Transactions on Antennas and Propagation*, vol. 65, no. 2, pp. 442–452, 2016.

[10] S. Taravati, "Aperiodic space-time modulation for pure frequency mixing," *Physical Review B*, vol. 97, no. 11, p. 115131, 2018.

[11] J. R. Zurita-Sánchez, P. Halevi, and J. C. Cervantes-González, "Reflection and transmission of a wave incident on a slab with a time-periodic dielectric function $\epsilon(t)$," *Physical Review A*, vol. 79, no. 5, p. 053821, 2009.

[12] D. Sarkar, *FDTD Analysis of Guided Electromagnetic Wave Interaction with Time Modulated Dielectric Medium*. Springer, 2022.

[13] A. Kumar and D. Sarkar, "FDTD analysis of space-time metamaterials using modulated tvtls for frequency translation, mixing and non-reciprocity," in *2023 53rd European Microwave Conference (EuMC)*. IEEE, 2023, pp. 311–314.

[14] P. Tien and H. Suhl, "A traveling-wave ferromagnetic amplifier," *Proceedings of the IRE*, vol. 46, no. 4, pp. 700–706, 1958.

[15] S. Qin, Q. Xu, and Y. E. Wang, "Nonreciprocal components with distributedly modulated capacitors," *IEEE Transactions on Microwave Theory and Techniques*, vol. 62, no. 10, pp. 2260–2272, 2014.

[16] A. Kumar, J. C. Dash, and D. Sarkar, "Computational techniques for design and analysis of time-varying capacitor loaded transmission lines using FDTD and simulink," *IEEE Journal on Multiscale and Multiphysics Computational Techniques*, vol. 7, pp. 228–235, 2022.

[17] ——, "FDTD analysis of transmission line loaded with time-varying shunt capacitors for mixer applications," in *2022 IEEE International Conference on Electronics, Computing and Communication Technologies (CONECCT)*. IEEE, 2022, pp. 1–6.

[18] D. M. Pozar, *Microwave Engineering*. John Wiley & Sons, 2011.

[19] *Advanced Design System 2011.01 - Harmonic Balance Simulation*, Agilent Technologies, Feb. 2011.